

QCD PHASE TRANSITION IN THE LABORATORY AND IN THE EARLY UNIVERSE

BIKASH SINHA

Variable Energy Cyclotron Centre and Saha Institute of Nuclear Physics, 1/AF Bidhan Nagar, Calcutta 700 064 (India)

(Received 29 October 1999; Accepted 29 May 2000)

The relativistic Fokker-Planck equation is used to study the evolution of the quark distribution in the quark gluon phase expected to be formed in ultra-relativistic heavy ion collisions. We find that though kinetic equilibrium is achieved by the light quark species, they fail to equilibrate chemically. The photon spectra produced from a hot hadronic gas is evaluated taking into account the in-medium modifications of hadronic properties. A phenomenological model of hadronic interactions is considered for this purpose. The possible footprints of the primordial quark hadron phase transition in today's universe are discussed. The possibility of quark nuggets being candidates for the baryonic component of cosmic dark matter is investigated.

Key Words: Quark Gluon Plasma; Successive Equilibrium; Photons; Quark Nuggets

1 Introduction

It is expected that two nuclei colliding at ultra-relativistic energies (~ 200 GeV/nucleon or more) may lead to hadronic matter go through a phase transition to its fundamental constituents, quarks and gluons, usually referred to as quark gluon plasma (QGP). Somewhat analogously, the universe, as per conventional wisdom should have consisted of quarks, gluons, leptons and photons, a microsecond after the Big Bang. The experience and wisdom, expected from nucleus-nucleus collisions in the laboratory are anticipated to facilitate our understanding of the quark-hadron phase transition. Indeed what possible footprints of that primordial epoch can be traced in today's cosmos is one of the interesting and intriguing questions (Fig. 1).

We focus¹ on electromagnetic signals in the laboratory experiments. photons and dileptons in particular. One found that using the simplest possible thermal model of a first order phase transition there is a hint of the existence of the QGP, although the limits of the thermal photon data necessarily imply that a confident prediction is not possible yet². With raw data of thermal photons coming out of lead-lead experiment at CERN³ the scenario looks promising although a lot more work needs to be done to come to a definitive conclusion. Similarly, the "mysterious" bump in the

dilepton data of CERES and HELIOS do not seem to get explained that easily, QGP or otherwise⁴.

Clearly, an understanding of the nature of the phase transition still remains an open question. Our lattice colleagues⁵ tell us that for a pure $SU(N)$ gauge the phase transition is second order for $N = 2$ and first order for $N = 3$. Introducing the fermions, the quarks, say u , d and s the scenario changes. For $N_f \geq 3$, the phase transition is of first order, but continuous for $N_f = 2$. Using the non-equilibrium statistical mechanics and QCD it can be shown that thermal equilibrium is a

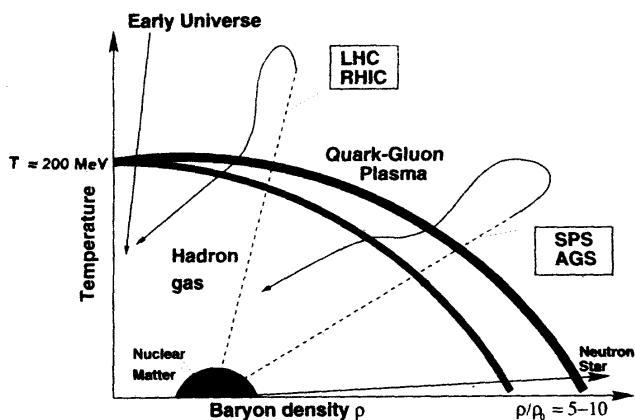


Fig. 1 QCD phase diagram

possibility, however, chemical equilibrium is probably not achieved.

Indeed at initial time, whatever that is ($\tau \sim 1$ fm) it is unlikely that a pure QGP is formed, whereas a mixture of quark bubbles with hot hadronic matter is a possibility. The initial boundary conditions which drive the space time evolution of the system is another area of intense discussion. Bjorken's simple scaling law⁶ is certainly not valid, transverse expansion is a reality.

Other research scientists⁷ who deal with Parton Cascade Model (PCM) seem to have considerable insight on just these questions. There is now a real possibility that we can build simple models based on the distilled wisdom of Cascades.

In this paper, the following areas have been covered : (1) The issue of successive thermal and chemical equilibrium scenarios (2) A detailed study of hot hadronic matter and its implication on the thermal model and finally (3) the surviving quark nuggets beyond a critical baryon content, and, nuggets being possible candidates for baryonic dark matter in the universe, a much more straightforward candidate than illusive axions or SUSY particles. It is our considered view that quark hadron phase transition in the microsecond universe is a thriving area of research and lot more can be understood and known from this primordial event.

2 Approach to Equilibrium

The primary motivation to study the non-equilibrium evolution of the quark-gluon system is driven from the fact that the characteristic time scales for the partonic processes are of the order of the lifetime of the *putative* QGP. Even if the system achieves thermodynamic equilibrium at some point of time, the study of the pre-equilibrium aspects is important to evaluate in the sense that the pollutants from this era may affect the kinematical domains where one looks for the signals of QGP. QGP diagnostics rely quite heavily on the phase space topology and distributions of quarks and gluons. To what extent equilibrium is achieved should obviously affect these signals.

To this end, the mechanisms governing the approach to thermalisation in the quark-gluon system have been a very topical issue of late^{7,8}.

The central theme of our approach is to exploit the well-known result⁹ that gg cross-section is considerably

larger than qg or qq cross-sections, primarily because of the colour factor of gluons. It is therefore reasonable to expect that the gluons would thermalise among themselves appreciably earlier than the whole system of quarks, antiquarks, and gluons. The proper time τ_g at which the gluons equilibrate is thus considerably less¹⁰ than the overall equilibration time τ_o ; the value of τ_o was proposed to be of the order of 1fm/c by Bjorken⁶ some time ago.

The gluons carry about 50% of the momentum and sea quarks only a tiny fraction. Thus, in very high energy collisions (RHIC or LHC energies), *if we confine our attention to the central rapidity region*, it is quite natural that from τ_g onwards, the equilibrated gluons may provide a thermal heat bath for the sea quarks (anti-quarks). This picture is further justified by the fact that the sea quark (antiquark) density is very low compared to that of the gluons in this region¹¹. Thus we are left with a system where a relatively small mixture of non-equilibrium degrees of freedom (quarks and antiquarks) interact with some equilibrated degree of freedom (the 'gluonic' bath); such processes are known to give rise to Brownian motion which is governed by the Fokker-Planck (FP) equation. QCD being asymptotically free, hard collisions involving large momentum transfers are suppressed compared to soft interactions and in our picture, thermalisation in the quark-gluon system proceeds through many such soft collisions. The FP equation describes, semi-classically, the evolution of the many body quark-gluon system in a kinetic theory framework. The system under consideration is highly relativistic and presumably at high temperatures. Therefore, production and annihilation of $q\bar{q}$ pairs in the gluonic heat bath must be taken into account. The relativistic FP equation with these effects can be written as (see ref. [12] for derivation),

$$\frac{\partial f}{\partial t} - \frac{\partial}{\partial p_z} \left(\frac{a p_z^p f}{\sqrt{p_z^2 + m_T^2}} \right) - D_F \frac{\partial f}{\partial p_z^2} = - \frac{f - f_{eq}}{\tau_{relax}} \dots (1)$$

where f_{eq} is the equilibrium distribution and τ_{relax} is the relaxation time estimated from the reactions $gg \leftrightarrow q\bar{q}$ and $g \leftrightarrow q\bar{q}$, m_T is the transverse mass

($= \sqrt{p_T^2 + m_{eff}^2}$). m_{eff} is the effective mass defined as

$m_{eff} = \sqrt{m_{current}^2 + m_{thermal}^2}$, $m_{current}$ is the current

quark mass (= 10MeV for u and d quarks) and $m_{thermal}$

is the thermal mass: $m_{thermal} = \sqrt{g_s^2 T^2 / 6}$ g_s is the

strong coupling constant. In a chemically non-equilibrated scenario, the thermal mass is replaced¹³ by

$m_{thermal}^2 = (1 + r_q / 2) g_s^2 T^2 / 9$ where r_q is the ratio of

equilibrium to non-equilibrium density. We have seen¹⁴ that the effect of such a change on thermal mass has negligible effects on the final results.

It should be noted that the reactions $g g \leftrightarrow g g g \dots$ etc. do not appear explicitly as the gluons have been assumed to be thermalized so that their density is determined from the temperature of the bath. Also, the thermal mass of the gluons is an essential ingredient; otherwise the reaction $g \leftrightarrow q\bar{q}$ would be forbidden.

2a Cooling of the Gluonic Heat Bath

The gluonic heat bath is cooling due to expansion and the rate of cooling is determined by the relativistic hydrodynamics. The bulk properties of the system, *e.g.* the cooling law etc., are governed by the equilibrated degrees of freedom. In our case the cooling is given by the Bjorken's scaling law with appropriate modification due to quark production through thermal gluon fusion $gg \leftrightarrow q\bar{q}$ and thermal gluon decay $g \rightarrow q\bar{q}$. We have obtained the cooling law¹⁴ by solving the hydrodynamic equation which is parametrised as $T = \alpha \tau^\beta$ where $\alpha = 0.4077$, $\beta = 0.355$ at LHC and $\alpha = 0.33$, $\beta = 0.352$ at RHIC energies respectively. The cooling rate in Bjorken model ($\beta = 1/3$) is slower compared to the present case where the production of quarks cost some energy.

2b Solution of the Fokker-Planck Equation

We solve the FP equation with the following initial and boundary conditions for a quark species j

$$f_j(p_z, \tau) \xrightarrow{\tau \rightarrow \tau_g} \Delta_j \delta(p_z) \quad \dots(2)$$

and

$$f_j(p_z, \tau) \xrightarrow{|p_z| \rightarrow \infty} 0 \quad \dots(3)$$

The parameter Δ_j is determined from the initial density of the partons. $\delta(p_z)$ is a rather good approximation of the low x structure function¹⁵. We should also mention here that the final outcome of the model is insensitive to the functional form of the initial distribution function - a typical characteristic of the Markovian process.

It is important to mention here that the final outcome depends on the value of Δ_j . There is a lack of consensus about the initial value of the quark density. We take the initial values of quark densities from HIJING¹⁶. The phase-space density of quark is larger in case of parton cascade model¹⁷ as also in the work of Shuryak¹¹. In this sense our work corresponds to a conservative situation. The data from RHIC and LHC should make a distinction among various models.

As mentioned earlier, in the system under study the quark density changes with proper time due to two mechanisms. The expansion dynamics (flow) dilutes the density and on the other hand, the creation of quarks in the relativistic heat bath enhances the quark density. The gluon density decreases due to expansion only. We calculate the ratio of the width of the distribution in non-equilibrium and equilibrium

situations, *i.e.* $\langle p_z^2 \rangle^{non-eq} / \langle p_z^2 \rangle^{eq}$. The advantage of calculating the ratio is that the expansion effects will get cancelled to some extent, though the cooling in the equilibrium and non-equilibrium scenario is different as has been mentioned before.

In Fig. 2, we plot these ratios as a function of the proper time τ . At RHIC (LHC) the initial thermalisation time, τ_g for the gluons is 0.3 fm/c (0.25 fm/c), the temperature $T_g(\tau_g)$ is 500 MeV (660 MeV) and the initial quark density n_{uid} is 0.7 fm⁻³ (2.8 fm⁻³). At RHIC energy (Fig. 2a) we observe that the ratio D saturates to a value ~ 1 , at a proper time $\tau \sim 3$ fm/c, well before

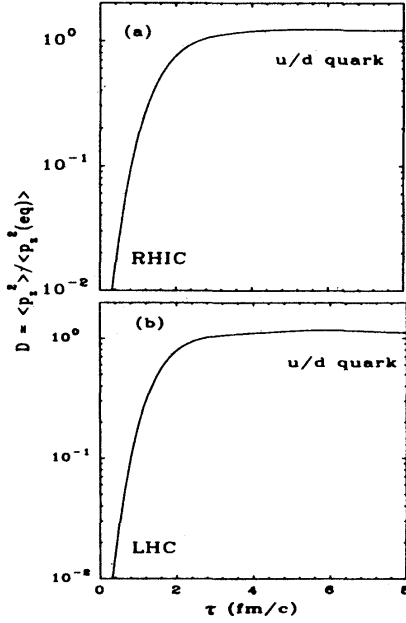


Fig. 2 Ratio of the width of the distribution in non-equilibrium and equilibrium situations are plotted as a function of τ for RHIC and LHC

the temperature of the system reaches to T_c (~ 160 MeV). In Fig. 2(b) we plot D for LHC energies; the thermal equilibration is complete within the proper time ~ 2 fm/c.

We evaluate the density of quarks in the non-equilibrium scenario by integrating the distribution function $f(p_\tau, \tau) G(p_\tau)$ over its momentum. The non-equilibrium density n_q has an explicit dependence on τ and an implicit dependence on τ through $T(\tau)$. But the equilibrium density $n_{eq}(T)$ has only an implicit dependence on t through $T(\tau)$. The ratio $r_q = n(\tau)/n_{eq}(T(\tau))$ thus assumes an *universal* feature, since the implicit time dependence gets eliminated. The time dependence of the ratio r_q can then be used as a ready marker for chemical equilibrium; the time at which the explicit time dependence of r_q vanishes, simultaneously with $r_q \rightarrow 1$, corresponds to the time for chemical equilibration for the flavour q . We observe from Fig. (3) that r_q neither saturates nor approaches the value unity before the temperature of the system reaches the value T_c (160 MeV). Therefore, we conclude that the chemical equilibrium is not achieved in the quark gluon system, although thermal (kinetic) equilibrium is

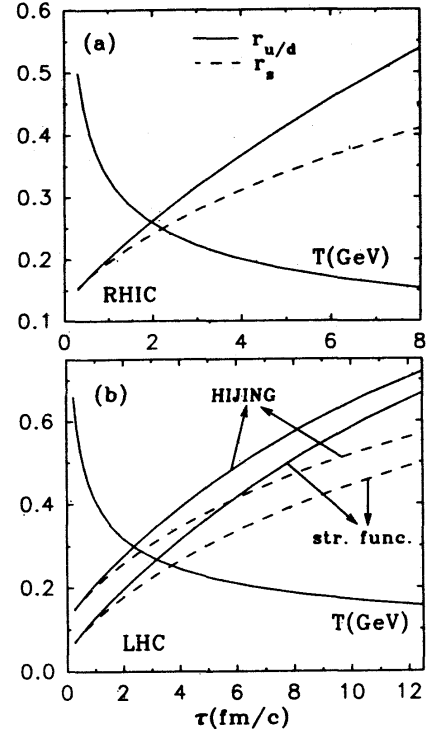


Fig. 3 Plot of r_q as a function of τ .

there. To show the sensitivity of the evolution of r_q on the initial quark density we show, in Fig. (3), the result of our calculations¹⁴ obtained by taking initial quark density from the structure functions^{10,15}. For the sake of completeness we also show the cooling law in Fig. 3, where $q\bar{q}$ production has been taken into account.

We have analysed the approach to thermal and chemical equilibrium in a quark gluon system within the framework of a semi-classical, physically transparent model. A fundamental consequence of this picture is that while thermal (kinetic) equilibrium is probable, chemical equilibrium is not, even for LHC energies. Even the kinetic equilibrium is achieved through a succession of time scales.

3 Photons from Hot Hadronic Matter

Whether a QCD phase transition takes place or not, photons can be used as a probe to study the properties of hadrons in hot/dense medium. In a phase transition scenario, apart from the QGP, photons are also produced from the thermalised hadronic gas, formed after the

phase transition (see ref. [17] for details). Substantial contributions to the total photon yield also come from the initial hard collision of partons in the high momentum regime, and from hadronic decays ($\pi^0 \rightarrow \gamma$, $\eta \rightarrow \gamma$ etc.) in the low momentum zone. The hard QCD photons can be well understood through perturbative QCD and the decay photons can be reconstructed by invariant mass analysis. Thus, to extract photon signals from QGP it is essential to estimate the photon rates from various hadronic reactions and vector meson decays which is a challenging task, indeed. The temperature of the hadronic phase lies between 150 - 200 MeV. Therefore the finite temperature corrections to the hadronic properties and their consequences on photon spectra are very important.

For our purpose, we model the hadronic gas as consisting of π , ρ , ω and η . First we consider the reactions $\pi\pi \rightarrow \rho\gamma$, $\pi\rho \rightarrow \pi\gamma$ and the decay $\rho \rightarrow \pi\gamma$. We estimate the differential cross-section for photon production from the above processes taking into account the finite width of the rho meson (see ref. [18] for details.) The relevant vertices are obtained from the following Lagrangian:

$$\mathcal{L} = -g_{\rho\pi\pi} \rho^{\rightarrow\mu} \cdot (\vec{\pi} \times \partial_\mu \vec{\pi}) - eJ^\mu A_\mu + \frac{e}{2} F^{\mu\nu} (\vec{\rho}_\mu \times \vec{\rho}_\nu)_3, \quad \dots(4)$$

where $F_{\mu\nu} = \partial_\mu A_\nu - \partial_\nu A_\mu$, is the Maxwell field tensor and J^μ is the hadronic part of the electromagnetic current given by

$$J^\mu = (\vec{\rho}_\nu \times \vec{B}^{\nu\mu})_3 + (\vec{\pi} \times (\partial^\mu \pi + g_{\rho\pi\pi} \vec{\pi} \times \rho^{\rightarrow\mu}))_3 \quad \dots(5)$$

with $\vec{B}_{\mu\nu} = \partial_\mu \vec{\rho}_\nu - \partial_\nu \vec{\rho}_\mu - g_{\rho\pi\pi} (\vec{\rho}_\mu \times \vec{\rho}_\nu)$, and the subscript 3 after the cross product indicates the relevant component in isospin space.

We have also considered the photon production due to the reactions $\pi\eta \rightarrow \pi\gamma$, $\pi\pi \rightarrow \eta\gamma$ and the decay $\omega \rightarrow \pi\gamma$ (see ref. [18] for details).

In the case of nuclear collisions, one is more interested in overall photon rates rather than the cross-sections. Using independent particle approximation of kinetic theory¹⁹ we can write down the rate of photon production per unit volume at a temperature T as

$$E \frac{dR}{d^3p} = \frac{1}{16(2\pi)^7 E} \int_{(m_1+m_2)^2}^{\infty} ds \int_{t_{min}}^{t_{max}} dt |\mathcal{M}|^2 \int dE_1 \times \int dE_2 \frac{f(E_2)f(E_2)[1+f(E_3)]}{\sqrt{aE_2^2 + 2bE_2 + c}} \quad \dots(6)$$

where \mathcal{M} is the invariant transition amplitude of photon production for the appropriate reaction channel, evaluated from the Lagrangians given by eq. (4). (For the parameters a , b , c please refer to [18]).

3a VNN Interaction

To calculate the effective mass and decay widths we begin with the following VNN (Vector - Nucleon - Nucleon) Lagrangian density:

$$\mathcal{L}_{VNN} = g_{VNN} \left(\bar{N}_{\gamma\mu} \tau^a N V_a^\mu - \frac{k_V}{2M} \bar{N} \sigma_{\mu\nu} \tau^a N \partial^\nu V_a^\mu \right), \quad \dots(7)$$

where $V_a^\mu = \{\omega^\mu, \rho^{\rightarrow\mu}\}$, M is the free nucleon mass.

N is the nucleon field and $\tau_a = \{1, \vec{\tau}\}$. The values of the coupling constants g_{VNN} and k_V will be specified later. With the above Lagrangian we proceed to calculate the ρ -self energy.

$$\Pi_{\mu\nu} = -2ig_{VNN}^2 \int \frac{d^4p}{(2\pi)^4} K_{\mu\nu}(p, k) \quad \dots(8)$$

with,

$$K_{\mu\nu} = \frac{\text{Tr}[\Gamma_\mu(k)(p+M^*)\Gamma_\nu(-k)(p-k+M^*)]}{(p^2 - M^{*2})((p-k)^2 - M^{*2})} \quad \dots(9)$$

The vertex $\Gamma_\mu(k)$ is calculated by using the Lagrangian of eq. (7) and is given by

$$\Gamma_\mu(k) = \gamma_\mu + \frac{ik_V}{2M} \sigma_{\mu\alpha} k^\alpha \quad \dots(10)$$

Here M^* is the in-medium (effective) mass of the nucleon at finite temperature which we calculate using the Mean-Field Theory (MFT)²⁰. The value of M^* can be found by solving the following self consistent equation:

$$M = M - \frac{4g_\sigma^2}{m_\sigma^2} \times \int \frac{d^3p}{(2\pi)^3} \frac{M^*}{(p^2 + M^{*2})^{1/2}} [f_N(T) + f_{\bar{N}}(T)], \quad \dots(11)$$

where $f_N(T)$ ($f_{\bar{N}}(T)$) is the Fermi-Dirac distribution for the nucleon (antinucleon), m_σ is mass of the neutral scalar meson (σ) field, and, the nucleon interacts via the exchange of isoscalar meson with coupling constant g_σ . Since the exact solution of the field equations in QHD is untenable, these are solved in mean field approximation. In a mean field approximation one replaces the field operators by their ground state expectation values which are classical quantities; this renders the field equations exactly solvable.

The vacuum part of the ρ self energy arises due to its interaction with the nucleons in the Dirac sea. This is calculated using dimensional regularization scheme.

In a hot system of particles, there is a thermal distribution of real particles (on shell) which can participate in the absorption and emission process in addition to the exchange of virtual particles. The interaction of the rho with the onshell nucleons, present in the thermal bath contributes to the medium dependent part of the ρ -self energy. This is calculated from eq. (8) using imaginary time formalism as,

$$\begin{aligned} \text{Re}\Pi_{\mu\nu d}(\omega, \mathbf{k} \rightarrow 0) &= \frac{16g_{\rho NN}^2}{\pi^2} \int \frac{p^2 dp}{\omega_p (e^{\beta\omega_p} + 1)(4\omega_p^2 - \omega^2)} \\ &\times \left[\frac{1}{3}(2p^2 + 3M^{*2}) - \omega^2 \left\{ M^* \left(\frac{k_\nu}{2M} \right) \right. \right. \\ &\left. \left. - \frac{1}{3} \left(\frac{k_\nu}{2M} \right)^2 (p^2 + 3M^{*2}) \right\} \right] \quad \dots(12) \end{aligned}$$

where, $\omega_p^2 = p^2 + M^{*2}$.

3b Finite Temperature Properties

In this section, we present the results of our calculation of the effective masses and decay widths of

vector mesons. In Fig. 4, we show the variation of the ratio of effective mass to free mass for hadrons as a function of temperature. For our calculations of ρ and ω mesons effective masses we have used the following values of the coupling constant and masses²¹:

$$\begin{aligned} k_\rho &= 6.1, \quad g_{\rho NN}^2 / 4\pi = 0.55, \quad m_\sigma = 550 \text{ MeV}, \quad m_\rho = 770 \text{ MeV} \\ M &= 938 \text{ MeV}, \quad g_\sigma^2 / 4\pi = 9.3, \quad g_{\omega NN}^2 / 4\pi = 20, \\ &\text{and } k_\omega = 0. \end{aligned}$$

Many authors have investigated the issue of temperature dependence of hadronic masses within different models over the past several years. Hatsuda and collaborators²²⁻²⁴ and Brown²⁵ showed that the use of QCD sum rules at finite temperature results in a temperature dependence of the $q\bar{q}$ condensate culminating in the following behaviour of the ρ -mass:

$$\frac{m_\rho^*}{m_\rho} = \left(1 - \frac{T^2}{T_x^2} \right)^{1/6} \quad \dots(13)$$

where T_x is the critical temperature for chiral phase transition. Brown and Rho²⁶ also showed that the requirement of chiral symmetry yields an approximate scaling relation between various effective hadron masses,

$$\frac{M^*}{M} \approx \frac{m_\rho^*}{m_\rho} \approx \frac{m_\omega^*}{m_\omega} \approx \frac{f_\pi^*}{f_\pi} \quad \dots(14)$$

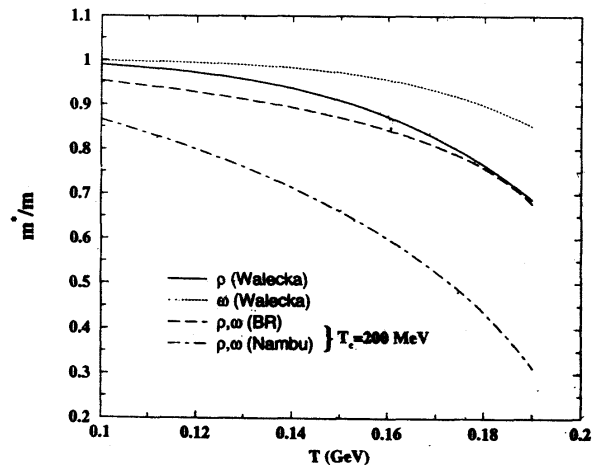


Fig. 4 Ratio of effective mass to free space mass of hadrons as a function of temperature T

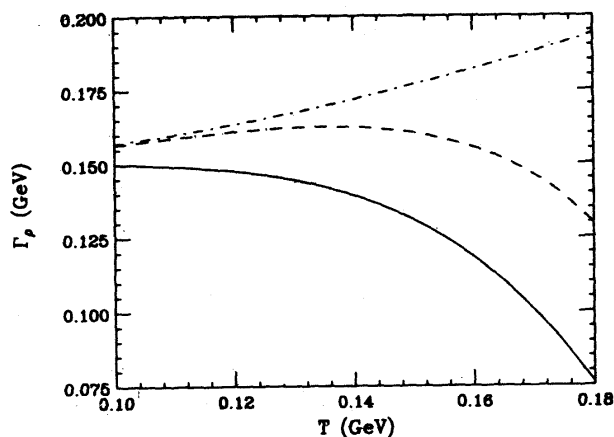


Fig. 5 Rho decay width (Γ_ρ) as a function of temperature (T). Dashed and solid lines show calculations of rho width with effective mass due to nucleon loop, with and without BE. Dot dashed line represents the same but with effective mass due to pion loop

These calculations show a dropping of hadronic mass with temperature. Calculations with non-linear σ -model, however, predict the opposite trend²⁷. The expected trend based on Brown - Rho scaling is also shown. Firstly, we do not observe any global scaling behaviour. Secondly, in our case the effective mass as a function of temperature falls at a slower rate.

The variation of the in-medium decay width (Γ_ρ) of the rho meson with temperature is shown in Fig. 5. As discussed earlier, the effective mass of the rho decreases as a result of $N\bar{N}$ polarisation. This reduces the phase space available for the rho. Hence, we observe a rapid decrease in the rho meson width with temperature (solid line). However, the presence of pions in the medium would cause an enhancement of the decay width through induced emission. Thus when Bose Enhancement (BE) of the pions is taken into account the rho decay width is seen to fall less rapidly (dashed line); such a behaviour is observed quite clearly in ref. [28]. For the sake of completeness, we also show the variation of rho width in the case where the rho mass changes due to $\pi\pi$ loop. In this case, since the rho mass increases (though only marginally), the width increases (dot-dashed line).

3c Photon Spectra

In this section, we present our results on photon emission rates from a hot hadronic gas. As discussed earlier, the variation of hadronic decay widths and

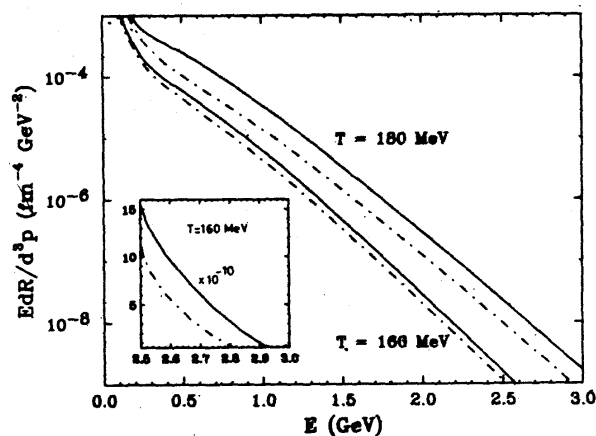


Fig. 6 Total photon emission rate from hot hadronic matter as a function of photon energy at $T = 160, 180$ MeV. The solid and dot-dashed lines show results with and without in-medium effects respectively. *Inset*: Total photon emission rate is plotted in linear scale as a function of photon energy in the kinematic window, $E_\gamma = 2.5$ to 3.0 GeV at $T = 180$ MeV

masses will affect the photon spectra. The relevant reactions of photon production are $\pi\pi \rightarrow \rho\gamma$, $\pi\rho \rightarrow \pi\gamma$, $\pi\pi \rightarrow \eta\gamma$, and $\pi\eta \rightarrow \eta\gamma$ with all possible isospin combinations. Since the lifetimes of the rho and omega mesons are comparable to the strong interaction time scales, the decays $\rho \rightarrow \pi\pi\gamma$ and $\omega \rightarrow \pi^0\gamma$ are also included. The effect of finite resonance width of the rho meson in the photon production cross-sections has been taken into account through the propagator.

In Fig. 6, we display the total rate of emission of photons from hot hadronic gas including all hadronic reactions and decays of vector mesons. At $T = 180$ MeV, the photon emission rate with finite temperature effects is a factor of ~ 3 higher than the rate calculated without medium effects. At $T = 160$ MeV the medium effects are small compared to the previous case.

We have calculated the effective masses and decay widths of vector mesons propagating in a hot medium. We have seen that the mass of rho meson decreases substantially due to its interactions with nucleonic excitations and it increases only marginally (~ 10 - 15 MeV) due to $\rho - \pi$ interactions. The overall decrease in the effective mass is due to fluctuations in the Dirac sea of nucleons with mass M^* and the in-medium contribution decreases very little (~ 5 - 10 MeV) from

its free space value. For ω mesons the in-medium contribution decreases by 80 MeV at $T = 180$ MeV but the Dirac sea effect is more prominent than the medium effect. The omega mass drops at $T = 180$ MeV by about 280 MeV from its free space value. Such changes in the properties of the vector mesons in hot and dense hadronic matter, as produced in heavy ion collisions, lead to the intriguing possibility of the opening of the decay channel $\omega \rightarrow \rho \pi$, for the omega meson, which is impossible in free space. This along with the channel $\omega \pi \rightarrow \pi \pi$ would result in a decrease in its effective life-time enabling it to decay within the hot zone and act as a chronometer in contribution to the commonly held opinion and would have implications in determining the size of the region using pion interferometry. A new peak and a radically altered shape of the low invariant mass dilepton spectra appears due to different shift in the masses of ρ and ω mesons.

We have evaluated the rate of photon emission from a hadronic gas of π , ρ , ω and η mesons. It is seen that the photon rate increases by a factor ~ 3 due to the inclusion of in-medium masses at $T = 180$ MeV. We observe that the inclusion of in-medium decay widths in vector meson propagator has negligible effects on photon emission rates, although the effect of in-medium decay widths with BE is substantial for the dilepton yield²⁸.

4 Quark Nuggets as Baryonic Dark Matter

According to the *standard model*, the universe underwent, a few microseconds after the big bang, a phase transition from quarks to hadrons. The cosmological implications of this, phase transition would be far-reaching. Schramm and collaborators²⁹ argued that for fluctuations in the horizon scale triggered by the phase transition may lead to the formation of primordial black holes, which could be as large as M_{\odot} , the solar mass. They recently suggested³⁰ that these black holes could even be the candidates for the Massive Compact Halo Objects (MACHO's)^{31,32}, which had of late been discovered in the halo of the Milky way, in the direction of the Large Magellanic Cloud (LMC) using the gravitational lensing techniques. On the other hand, a first order phase transition scenario involving bubble nucleation at a critical temperature $T_c \sim 100 - 200$ MeV could lead to the formation of quark nuggets (QN)³³, made of u , d and s quarks at a

density $>$ nuclear density. If these primordial QN's existed till the present epoch, they could be possible candidates for the dark matter³³.

The central question in this context then is whether the primordial QN's can be stable on a cosmological time scale. In a recent work³⁴ using the chromo-electric flux tube model, we have demonstrated that the QN's will survive against baryon evaporation, if the baryon number of the quark matter inside the nugget is larger than 10^{42} . It should be noted at this point that the horizon limit on the baryon number at that primordial epoch is around 10^{49} . The conclusion from these calculations is that the larger primordial QN's within the baryon number window $10^{42} \leq N_B \leq 10^{49}$ are indeed cosmologically stable. It is therefore most relevant to ask what fraction of the dark matter could be accounted for by the surviving QN's in the mass window just mentioned. Thus, we wish to address the question whether the proverbial cosmological dark matter, containing 90% or more of all the matter in the universe, can be made up entirely of such QN's.

It is well known that in a first order phase transition, the quark and the hadron phases co-exist in a mixed phase. Around the critical temperature, the universe consists of leptons, photons and the massless quarks, anti-quarks and gluons, described by the MIT bag model with an effective degeneracy $g_q (\sim 51.25)$. Note that the baryon number in this phase is carried entirely by the quarks. The hadronic phase contains baryons, mesons, photons and leptons and is described by an equation of state corresponding to massless particles with an effective degeneracy $g_h = 17.25$.

In the usual picture of bubble nucleation in first order phase transitions, hadronic matter starts appearing in the quark matter as individual bubbles. With the progress of time, more and more hadronic bubbles form, coalesce and eventually percolate to form a network of hadronic bubbles form, coalesce and eventually percolate to form a network of hadronic matter which traps the quark phase into finite domains³⁵. The time when the percolation takes place is usually referred to as the percolation time t_p , determined by a critical volume fraction of the QGP, f_c , ($f_c \equiv f(t_p)$) of the quark phase (see ref. [36] for details).

Detailed numerical studies on percolating systems yield the result that for bubbles with the same radial

size, f_c is $\sim 0.3^{37,38}$. We would also use the same value of f_c here. For the sake of simplicity, we would also assume that the trapped quark domains are all of the same size.

In an ideal first order phase transition, the fraction of the high temperature phase decreases from the critical value f_c , as these domains shrink. For the QCD phase transition, however, these domains should become QN's and as such, we may assume that the lifetime of the mixed phase t_f (i.e., the time when the cooling due to expansion starts to dominate again and the temperature of the universe starts falling), is $\sim t_p$.

The probability of finding a domain of trapped quark matter of co-ordinate radius X at time t_p is given by³⁵,

$$P(z, x_p) = \exp \left[-\frac{4\pi}{3} v^3 t_c^4 \int_{x_i}^{x_p} dx I(x) \times (zr(x) + y(x_p, x))^3 \right] \quad \dots(15)$$

where $z = X R(t_p)/vt_c$, $x = t/t_c$, $r(x) = R(x)/R(x_i)$ and $I(x)$ is the rate of nucleation per unit volume. v is the radial growth velocity of the nucleating bubbles, which we treat as a parameter. $y(x, x')$ is given by

$$y(x, x') = \int_{x'}^x r(x'')/r(x'') dx'' \quad \dots(16)$$

Various authors^{35,39-41} have proposed different nucleation rates for the cosmic QCD phase transition. We start with the nucleation rate given by delta function. The delta function nucleation rate can be realized by phase transition caused by impurities, like, primordial black holes, magnetic monopoles, relic abundances of the electroweak phase transition, or cosmic strings etc⁴².

In Fig. 7, we plot the probability $P(z, x_p)$ as a function of z . The radius of the trapped quark domain is determined by the length scale where the probability falls to f_c/e . This implies, $r_{QN}/vt_c \approx 0.019$.

The number density of the QN's (n_{QN}) can be obtained by using the relation $n_{QN} V_{QN} = f_c$, whence, $n_{QN} \approx 1968 / (vt_p)^3$.

In an idealised situation where the universe is closed by the baryonic dark matter trapped in the QN's, we should have,

$$N_B^H(t_p) = N_B^{QN} n_{QN} V^H(t_p) \quad \dots(17)$$

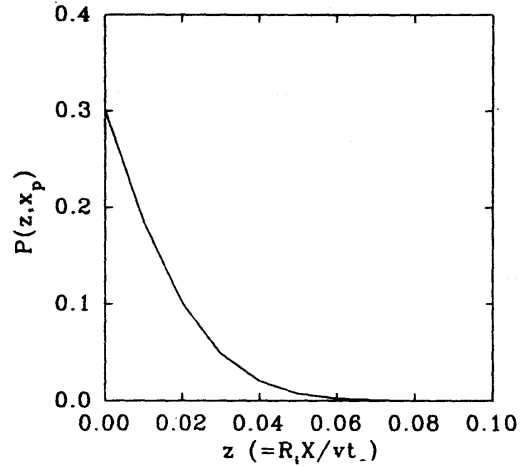


Fig. 7 Probability of finding a domain of co-ordinate size X in the quark phase at time t_p as a function of $R_i X/vt_c$ with the nucleation rate given by delta function.

where $N_B^H(t_p)$ is the total number of baryon required to close the universe ($\Omega_B = 1$) at t_p , N_B^{QN} is the total number of baryons contained in a single quark nugget and $V_H(t_p) = 4\pi (ct_p)^3/3$ is the horizon volume.

Demanding that $v/c \leq 1/\sqrt{3}$, we get

$$N_B^{QN} \leq 10^{-4.7} N_B^H(t_p) \quad \dots(18)$$

Since the usual baryons constitute only $\sim 10\%$ of the closure density, a total baryon number of 10^{50} within the horizon at a temperature of ~ 100 MeV would close the universe baryonically. This would require N_B^{QN} to be $\leq 10^{45.3}$, which is clearly within the survivability limit of QN's mentioned earlier.

In the nucleation scenario of Cottingham *et al.*³⁹ the density of QN's is found to be larger than the previous case $n_{QN} = 42947/(vt_p)^3$ and the corresponding limit on N_B^{QN} is given by $N_B^{QN} = 10^{-6} N_B^H(t_p)$. For $N_B^H(t_p) \sim 10^{50}$, N_B^{QN} to be $\leq 10^{44}$. With the nucleation scenario of refs. [40] and [41], $N_B^{QN} \leq 10^{44}$ and $10^{44.5}$, respectively, for the value of the surface tension = 50 MeV/fm². The final results are insensitive to the value of surface tension.

It thus appears that the upper limit on the baryon number of QN's that would close the universe baryonically is not very sensitive to the nucleation mechanism and all available estimates point to the real possibility that stable QN's could not only be a possible candidate for cold dark matter but they indeed can close the universe with total baryon numbers within the window mentioned earlier.

In order for the stable QN's to be a viable candidate for the cosmological dark matter, they must gravitationally clump, just like normal matter. It may however be asked what, if any, observational signatures could these stable QN's have at the present time. To this end, we may estimate the rate at which such QN's may collide with the earth, in the extreme case where all these QN's were floating around in the universe. For the various scenarios^{35,39-41} considered here, the rate of such collisions (density of QN's \times velocity of QN's ($v_{QN} \sim 2 \times 10^7$ cm/sec) \times surface area of the earth

($\sim 8 \times 10^{17}$ cm²)) turns out to be one in $\sim 10^{15} - 10^{16}$ years for $v = c/\sqrt{3}$.

More realistically, however, the scenarios proposed here would get substantial experimental support, *albeit* somewhat indirect, if a sizable flux of stable strangelets (heavy nuclear objects with very abnormal charge-to-mass ratios) could be detected in the cosmic rays. We may recall that there has been a report in the literature⁴³ that such objects may indeed form part of the extragalactic cosmic rays.

5 Acknowledgements

The author would like to thank J Alam, P Roy, S Sarkar and S Raha for their collaboration in the work reported here. The author would also like to dedicate this paper to the memory of his dear friend and colleague David Schramm, who is no more in this world.

References

- 1 B Sinha *Relativistic Aspects of Nuclear Collisions* (Eds. T Kodama *et al.*) World Scientific Singapore (1996)
- 2 D K Srivastava and B Sinha *Phys Rev Lett* **73** (1994) 2421
- 3 B Wyslouch *Quark Matter '97* Tsukuba Japan (1997)
- 4 D K Srivastava, B Sinha and C Gale *Phys Rev* **C53** (1994) R567
- 5 A Ukawa *Quark Matter '97* Tsukuba Japan (1997)
- 6 J D Bjorken *Phys Rev* **D27** (1993) 140
- 7 K Geiger *Phys Rep* **258** (1995) 237
- 8 X N Wang *Phys Rep* **280** (1997) 287
- 9 R Cutler and D Sivers *Phys Rev* **D17** (1978) 196
- 10 E Shuryak *Phys Rev Lett* **68** (1992) 3270
- 11 E Shuryak and L Xiong *Phys Rev Lett* **70** (1993) 2241
- 12 P Roy, J Alam, S Sarkar, B Sinha and S Raha *Nucl Phys* **A624** (1997) 687
- 13 C T Traxler and M H Thoma *Phys Rev* **C53** (1996) 1348
- 14 J Alam, P Roy, S Sarkar, S Raha and B Sinha *Int J Mod Phys* **A12** (1997) 5151
- 15 M Glück, E Reya and A Vogt *Z Phys* **C48** (1990) 471
- 16 T S. Biró, E van Doorn, B Müller, M H Thoma and X N Wang *Phys Rev* **C48** (1993) 1275
- 17 J Alam, S Raha and B Sinha *Phys Rep* **273** (1996) 243
- 18 S Sarkar, J Alam, P Roy, A Dutta-Mazumder, B Dutta-Roy and B Sinha *Nucl Phys* **A634** (1998) 206
- 19 C Gale and J I Kapusta *Phys Rev* **C35** (1987) 2107
- 20 B D Serot and J D Walecka *Advances in Nuclear Physics* **16** Plenum Press New York (1986)
- 21 R Machleidt, K Holinde and Ch ELster *Phys Rep* **149** (1987) 1
- 22 R J Furnstahl and T Hatsuda *Phys Rev* **D42** (1990) 1744
- 23 C Adami, T Hatsuda and I Zahed *Phys Rev* **D43** (1991) 921
- 24 T Hatsuda *Nucl Phys* **A544** (1992) 27c
- 25 G E Brown *Nucl Phys* **A522** (1991) 397c
- 25 G E Brown and M Rho *Phys Rev Lett* **66** (1991) 2720
- 27 A Bhattacharyya, J Alam, S Raha and B Sinha *Int J Mod Phys* **A** (in press)
- 28 A K Dutt-Majumdar, J Alam, B Dutta-Roy and B Sinha *Phys Lett* **B378** (1996) 35
- 29 M Crawford and D N Schramm *Nature* **298** (1982) 538
- 30 D N Schramm *Proc 3rd Int Conf Phys & Astrophys of Quark Gluon Plasma* Jaipur (India) (March 1997) (in press)
- 31 E Aubourg *et al.* *Nature* **365** (1993) 623
- 32 C Alcock *et al.* *Nature* **365** (1993) 621
- 33 E Witten *Phys Rev* **D30** (1984) 272
- 34 P Bhattacharjee, J Alam, B Sinha and S Raha *Phys Rev* **D48** (1993) 4630

- 35 H Kodama, M Sasaki, K Sato *Prog Theo Phys* **68** (1982) 1979
- 36 J Alam, S Raha and B Sinha *VECC-AST*
- 37 K Iso, H Kodama and K Sato *Phys Lett* **B169** (1986) 337
- 38 D Stauffer *Phys Rep* **54** (1979) 1
- 39 W N Cottingham, D Kalafatis and R Vinh Mau *Phys Rev Lett* **73** (1994) 1328
- 40 L D Landau and E M Lifshitz *Statistical Physics* Pergamon Press New York (1969)
- 41 K Kajantie *Phys Lett* **285B** (1992) 331
- 42 M B Christiansen and J Madsen *Phys Rev* **D53** (1996) 5446
- 43 T Saito, Y Hatano, Y Fukuda, H Oda *Phys Rev Lett* **65** (1990) 2094